THE JOURNAL OF BIOLOGICAL CHEMISTRY
Vol. 279, No. 31, Issue of July 30, pp. 32554–32561, 2004

Printed in U.S.A.

RNA Editing Generates Tissue-specific Sodium Channels with Distinct Gating Properties*

Received for publication, March 3, 2004, and in revised form, May 6, 2004
Published, JBC Papers in Press, May 10, 2004, DOI 10.1074/jbc.M402392200

Weizhong Song‡, Zhiqi Liu‡, Jianguo Tan, Yoshiko Nomura, and Ke Dong§

From the Department of Entomology and Neuroscience Program, Michigan State University, East Lansing, Michigan 48824

Sodium channels play an essential role in generating the action potential in eukaryotic cells, and their transcripts, especially those in insects, undergo extensive A-to-I RNA editing. The functional consequences of RNA editing of sodium channel transcripts, however, have yet to be determined. We characterized 20 splice variants of the German cockroach sodium channel gene *BgNa$_v$*. Functional analysis revealed that these variants exhibited a broad range of voltage-dependent activation and inactivation. Further analysis of two variants, BgNa$_v$1-1 and BgNa$_v$1-2, which activate at more depolarizing membrane potentials than other variants, showed that RNA editing events were responsible for variant-specific gating properties. Two U-to-C editing sites identified in BgNa$_v$1-1 resulted in a Leu to Pro change in segment 1 of domain III (IIIS1) and a Val to Ala change in IVS4. The Leu to Pro change shifted both the voltage dependence of activation and steady-state inactivation in the depolarizing direction. Two A-to-I editing events in BgNa$_v$1-2 resulted in a Lys to Arg change in IS2 and an Ile to Met change in IVS3. The Lys to Arg change shifted the voltage dependence of activation in the depolarizing direction. Moreover, these RNA editing events occurred in a tissue-specific and development-specific manner. Our findings provide direct evidence that RNA editing is an important mechanism generating tissue-/cell type-specific functional variants of sodium channels.

The voltage-gated sodium channel is responsible for the rising phase of the action potential in the membranes of neurons and other excitable cells (1). At least nine different mammalian sodium channel α-subunits (Na$_v$1.1 to Na$_v$1.9) have been identified (2, 3). These sodium channel isoforms exhibit distinct expression patterns in the nervous system and skeletal and cardiac muscle (4). Differences in electrophysiological properties have been observed among different mammalian sodium channel α-subunit isoforms, which likely contribute to their specialized functional roles in various tissues/cell types (4–6). In contrast to multiple sodium channel genes in mammals, there appears to be only one functional sodium channel gene in insects. For example, *para* is the only gene that encodes a functional sodium channel in *Drosophila melanogaster* (7–9). Orthologs of the *para* gene, house fly *Vssc1* and cockroach *BgNa$_v$* (formerly *para^{CSMA}*), have been cloned and characterized in *Xenopus* oocytes (10–12).

Alternative splicing and developmental regulation of alternative splicing have been documented in both mammalian and insect sodium channel genes (12–21). Conservation of splicing sites among mammalian and insect sodium channel strongly suggests the biological importance of alternative splicing. Indeed, significant modifications of functional properties of sodium channels by alternative splicing have been demonstrated (12, 19).

RNA editing is another important post-transcriptional modification that could significantly change protein functions by introducing site-specific alterations in gene transcripts, including the conversion of one base to another, or the insertion and deletion of nucleotides (22–24). Originally discovered in yeast tRNAs, A-to-I RNA editing has since been found in almost a dozen transcripts encoding ion channels and neurotransmitter receptors in the nervous system and also in multiple viral RNA transcripts (22). The best studied transcripts are subunits of mammalian glutamate-gated ion channels, a mammalian serotonin receptor (25, 26), and squid voltage-gated potassium channels (27, 28). In these cases, edited channels or receptors exhibit distinct functional and/or pharmacological properties. Ten A-to-I editing sites are found in the *para* transcript in *D. melanogaster* (29). However, the impact of RNA editing on sodium channel function remains elusive.

Here, we showed that tissue-specific RNA editing in the cockroach sodium channel mRNA modulates sodium channel gating properties, providing the first direct evidence for the involvement of RNA editing in post-transcriptional modification of sodium channels.

EXPERIMENTAL PROCEDURES

Cockroach Tissues—Ovary, gut, and leg and nerve cord tissues were isolated from insecticide-susceptible German cockroaches (CSMA). Nerve cords include thoracic ganglia, abdominal ganglia, and the connectives. For the analysis of developmental profile of *BgNa$_v$* transcripts, embryonic and immature stages were divided into the following five: embryonic stages I, II, and III, and nymph stages I and II. Embryos in embryonic stage I had uniform yolk and no obvious segmentation; stage II embryos had segmentation in abdomen and legs, but no eye coloration; and stage III embryos had very distinct eye color and well formed appendages and antennae. These three embryonic stages correspond to stages 1–5, stages 6–12, and stages 16–18, respectively, defined by Bell (30). The first and second nymphal instars were designated as nymph I and the last instar (6th) as nymph II.

Molecular Analysis—Total RNA was isolated from cockroach tissues, including head/thorax, leg, ovary, gut, and nerve cord, using TRIzol Reagent (Invitrogen). Methods for first-strand cDNA synthesis, reverse transcription-PCR, cloning, and PCR amplification of genomic DNA were identical to those described by Tan *et al.* (12). Primers used for the PCR analysis of optional exons and RNA editing sites are listed in Table I. Total RNA from heads and thoraces of four cockroaches (about 90 mg of tissue) was used to isolate partial cDNA clones for identification of

* This work was supported by National Science Foundation Grants IBN98081 and IBN0224877. The costs of publication of this article were defrayed in part by the payment of page charges. This article must therefore be hereby marked "*advertisement*" in accordance with 18 U.S.C. Section 1734 solely to indicate this fact.

‡ These authors contributed equally to this work.

§ To whom correspondence should be addressed: Dept. of Entomology, 106 Center for Integrated Plant Systems, Michigan State University, East Lansing, MI 48824. Tel.: 517-432-2034; Fax: 517-353-5598; E-mail: dongk@msu.edu.

TABLE I
Oligonucleotide primers used for this study

Primer[a]	Nucleotide sequence (5′–3′)	Amino acid position[b]	Exon or editing site
1	acgactcgtcctcaatctcag (→)[c]	3–9	J
2	aaaggccttgcattcggacag (←)	74–80	J
3	ctaccacaaccagagaac (→)	97–102	K
4	gcatgccagttctcatcattca (←)	302–309	K
5	gccatgtcctacgatgagttg (→)	417–423	I
6	cactagattttcctggtatg (←)		I
7	gcaagtttgagtctacc (→)	535–540	A
8	gctccatcatcactgtctgctgac (←)	674–681	A
9	gggtgcaggcaacaaatctca (→)	640–646	B
10	gggaaataatagatggagac (←)	728–734	B
11	ctatgtgggattgtatgcttgttg (→)	968–975	E
12	ccaactggaggagggtc (←)		E
13	acacggaccttgacctcac (→)	1068–1074	F
14	cttttcctccccatccatagtc (←)	1180–1186	F
15	aatcaagcgaagatgtgagattgcgccac	3′-UTR[d]	
16	tgaggacgtcatgatgtcag (→)	1221–1228	P/L
17	tgacagtgaagatacgatcc (←)	1308–1313	P/L
18	atcgtcatcttcagttccg (→)	1628–1633	V/A; L/M
19	tttcaccagacgcaggactcg (←)	1692–1698	V/A; L/M
20	ttcaacccgattcgacgggttgc (→)	127–134	K/R
21	aaggtacgtgaatggctgaag (←)	192–198	K/R

[a] Primers 1–14 were used to amplify alternative exons. Most of them correspond to sequences flanking these optional exons, except primers 6 and 12 designed based on alternative exon-specific sequences. Primer 15 was used in reverse transcription. Primers 16–21 were used in the analysis of RNA editing sites.
[b] The amino acid positions refer to those in the published sequence of *BgNa$_v$* (GenBank accession number: U73583).
[c] The sense and antisense primers are marked with → and ←, respectively.
[d] UTR, untranslated region.

RNA editing sites. The nucleotide sequences were determined at the Genomic Technology Service Facility at Michigan State University.

Site-directed mutagenesis was performed using the Altered Sites II *in vitro* Mutagenesis System (Promega, Madison, WI). BgNa$_v$1-1 has four amino acid changes: R502G, L1285P, V1685A, and I1806L (*e.g.* for R502G, Arg in the available sequence (GenBank accession number U73583) and Gly in BgNa$_v$1-1). BgNa$_v$1-2 also has four amino acid changes: R45G, K184R, I1663M, and N1787D. To determine which amino acid residue(s) contributed to the unique gating properties of BgNa$_v$1-1 and BgNa$_v$1-2, we replaced these residues individually with the corresponding residues in the published BgNa$_v$ sequence. Briefly, a 0.9-kb KpnI/SphI fragment containing Gly^{502} in BgNa$_v$1-1, Gly^{45} and Arg^{184} in BgNa$_v$1-2, a 1.4-kb Eco47III fragment containing Pro^{1285} and Ala^{1685} in BgNa$_v$1-1 and Met^{1663} in BgNa$_v$1-2, and a 1.7-kb HindIII fragment containing Leu^{1806} in BgNa$_v$1-1 and Asp^{1787} in BgNa$_v$1-2 were used for site-directed mutagenesis. We also generated BgNa$_v$1-1A from BgNa$_v$1-1 by changing all four amino acid resides to the corresponding ones in the published BgNa$_v$ sequence.

Expression of BgNa$_v$ Sodium Channels in Xenopus Oocytes—The procedures for oocyte preparation and cRNA injection are identical to those described by Tan *et al.* (12). For robust expression of the cockroach *BgNa$_v$* sodium channel, *BgNa$_v$* cRNA (0.2–2 ng) was coinjected into oocytes with *D. melanogaster tipE* cRNA (0.2–2 ng), which is known to enhance the expression of insect sodium channels in oocytes (8, 9).

Electrophysiological Recording and Analysis—Methods for electrophysiological recording and data analysis are similar to those described previously (12). The voltage dependence of sodium channel conductance (G) was calculated by measuring the peak current at test potentials ranging from −80 mV to +65 mV in 5-mV increments and divided by $(V - V_{rev})$, where V is the test potential and V_{rev} is the reversal potential for sodium ion. Peak conductance values were normalized to the maximal peak conductance (G_{max}) and fitted with a two-state Boltzmann equation of the form

$$G/G_{max} = (1 + \exp(V - V_{1/2})/k)^{-1} \quad \text{(Eq. 1)}$$

in which V is the potential of the voltage pulse, $V_{½}$ is the half-maximal voltage for activation, and k is the slope factor.

The voltage dependence of sodium channel inactivation was determined using 200-ms inactivating pre-pulses from a holding potential of −120 mV to 0 mV in 5-mV increments, followed by test pulses to −10 mV for 20 ms. The peak current amplitude during the test depolarization was normalized to the maximum current amplitude and plotted as a function of the pre-pulse potential. The data were fitted with a two-state Boltzmann equation of the form

$$I/I_{max} = (1 + (\exp(V - V_{1/2})/k))^{-1} \quad \text{(Eq. 2)}$$

in which I_{max} is the maximal current evoked, V is the potential of the voltage pulse, $V_{½}$ is the half-maximal voltage for inactivation, and k is the slope factor.

To determine the recovery from fast inactivation, sodium channels were inactivated by a 200-ms depolarizing pulse to −10 mV and then repolarized to −120 mV for an interval of variable durations followed by a 20-ms test pulse to −10 mV. The peak current during the test pulse was divided by the peak current during the inactivating pulse and plotted as a function of duration time between the two pulses. To determine the time constant for recovery, the curve was fitted using double exponential function

$$I = 1 - (A_1 * \exp(-t/\tau_1) + A_2 * \exp(-t/\tau_2)) \quad \text{(Eq. 3)}$$

where A_1 and A_2 are the relative proportions of current recovering with time constants τ_1 and τ_2, and t is recovery interval.

RESULTS

Identification of 20 Splice Types of the Cockroach Sodium Channel Gene—In a previous study, we reported the isolation and functional characterization of three cockroach BgNa$_v$ variants, KD1, KD2, and KD3 (12). These variants exhibit distinct gating and pharmacological properties (12). To elucidate the full complement of the BgNa$_v$ sodium channel diversity, we isolated 66 more full-length cDNA clones using the same cloning strategy in this study. Extensive restriction enzyme digestion of these clones revealed sequence polymorphism in several regions. Subsequent PCR sequencing analysis of these regions using PCR primers in Table I confirmed deletions or insertions of short segments, ranging from 19 to 129 bp in size. Because the locations and sequences of most insertions or deletions are homologous to the optional exons identified in the *Drosophila para* transcripts (16–18), these cockroach alternative exons are designated with the same letters, except in capitals (Fig. 1*A*). Most optional exons are located in the first or second intracellular linkers connecting domains I and II or domains II and III. High degrees of sequence homology are evident between *Drosophila* optional exons a and b and the corresponding cockroach exons A and B. Because exon A contains 19 nucleotides, exclusion of exon A results in frameshift, introducing a premature stop codon downstream in the first linker connecting domains I and II. Optional exon K is found only in cockroach and encodes

A

```
Exon a:  TSLSLPGSPFNIRRGSRSSHK
Exon A:  ASLSLP(a)------------
          *****
Exon b:  VSVYYFPT
Exon B:  VSIYYFPT
         ** *****
Exon e:  GERTNQISWIWSE
Exon E:  GE--GPSS-SWKE
         **     *  * *
Exon f:  -GKGVCRCISA
Exon F:  DAHE--RDTDLDLT
               *
Exon i:  V-SV--I-Q-RQPAPTTAHQAT-KVR-KVST
Exon I:        VPQFRDTKTATKSQFTFAYQENLVK
                 * *     *  * *
Exon j:  PRYGRKKKQKE
Exon J:  GDFGRRKKKKE
            ** ** **
Exon K:  VIFTGIYTFESAVKVMARGFILQPFTYLRDAWNWLDFVVIALA
```

B

Splice-type	J	K	I	A	B	E	F	G1	G2	G3	Clones (n)
1	+	+	−	+	−	−	+	+	−	−	38
2	−	+	+	+	−	−	+	−	+	−	1
3	+	+	−	+	−	+	+	−	−	+	1
4	−	+	+	+	−	+	+	+	−	−	1
5	+	+	+	+	−	−	+	+	−	−	2
6	+	+	−	+	−	+	+	+	−	−	6
7	+	+	−	+	−	−	−	+	−	−	1
8	−	+	−	+	−	+	+	+	−	−	1
9	−	+	−	+	−	−	+	+	−	−	2
10	−	+	−	+	+	−	+	+	−	−	2
11	−	+	−	+	−	−	+	−	+	−	1
12	−	−	−	+	−	−	+	+	−	−	1
13	−	−	−	+	+	+	+	+	−	−	1
14	+	−	−	+	+	−	+	+	−	−	1
15	+	+	−	+	+	−	+	+	−	−	3
16	+	+	−	+	+	+	+	+	−	−	2
17	−	+	−	+	+	−	+	+	−	−	2
18	−	+	−	+	+	−	+	−	+	−	1
19	−	+	−	+	−	−	+	+	+	−	1
20	+	+	−	−	−	−	+	+	−	−	1

FIG. 1. **Identification of 20 splice types of *BgNa$_v$*.** *A*, alignments of the deduced amino acid sequences encoded by alternative exons between *para* (*top*) and *BgNa$_v$* (*bottom*). The exon sequence alignment was performed using the DNAStar program. The *asterisks* underneath the sequences represent the sequence identity, and gaps introduced to obtain optimal alignments are indicated as *dashes*. Exon A contains 19 nucleotides (ggcaagtttgagtctacca). The last nucleotide "a" is presented in *parentheses*. *B*, usage of alternative exons in 69 full-length cDNA clones. The + and − *symbols* represent the presence and absence of an optional exon, respectively. Exons G1/G2/G3 are mutually exclusive, encoding IIIS3–4 (12). The variants are named according to the splice types. For example, the variants in splice type 1 are designated as BgNa$_v$1, and variants belonging to this splice type are named BgNa$_v$1-1 to BgNa$_v$1-38.

43 amino acid residues in IS2-3.[1]

Examination of the presence or absence of each alternative exon in the 69 full-length clones, including KD1, KD2, and KD3, revealed 20 splice types (Fig. 1*B*), which are far less than the possible random combinations of the identified alternative exons. This observation strongly suggests biased inclusion and exclusion of certain exons in sodium channels. In fact, 38 clones, including KD1, had the same splice type (Fig. 1*B*), which represents the most prevalent sodium channel splice type in the German cockroach. Hereinafter, we refer to the variants according to their splice types. For example, variants that belong to splice type 1 are named BgNa$_v$1-1, BgNa$_v$1-2, and so on. Therefore, KD1, KD2, and KD3 are renamed BgNa$_v$1-1, BgNa$_v$2, and BgNa$_v$3, respectively.

Sodium Channel Variants Exhibit Different Gating Properties—Variants BgNa$_v$1-1, BgNa$_v$2, and BgNa$_v$3 were characterized previously in oocytes, revealing distinct gating and pharmacological properties (12). In this study, we performed functional analysis of eighteen new variants including two type 1 variants (BgNa$_v$1-2 and BgNa$_v$1-3) and 16 variants each representing a unique splice type (BgNa$_v$5 to BgNa$_v$20). The electrophysiological properties of these variants were examined using two-electrode voltage clamp. 9 of 18 variants produced sufficient sodium currents for functional analysis (Table II), whereas the remaining 9 variants produced little or no sodium currents, possibly representing nonfunctional channels or channels that require additional cellular signals for robust expression. Sodium currents were completely blocked by tetrodotoxin at 10 nM for all functional splice variants except for BgNa$_v$11. BgNa$_v$11 exhibited a low level of resistance to TTX. At 10 nM, 60% of BgNa$_v$11 peak current was inhibited, and a concentration of 50 nM was required to block it completely.

All 9 functional variants activated rapidly in response to depolarization and then inactivated rapidly and nearly completely, similar to that reported for BgNa$_v$1-1 (12). To determine whether different variants exhibit different gating properties, the voltage dependence of activation, voltage dependence of steady-state inactivation, and recovery from fast inactivation were determined using the protocols described under "Experimental Procedures." The voltage for half-maximal activation ranged from −25 to −44 mV (Table II). BgNa$_v$11 activated at a more hyperpolarizing membrane potential, and BgNa$_v$1-1 and BgNa$_v$1-2 required larger membrane depolarization for activation. The remaining variants exhibited properties intermediate between these two extremes. A broad voltage range for half-maximal inactivation, from −37 to −54 mV, was evident among the variants (Table II). BgNa$_v$8 and BgNa$_v$11 inactivated at more negative membrane potentials than the others. There was no significant difference in kinetics of recovery from inactivation among the variants (Table II).

Optional Exon B Modulates Sodium Current Expression—9 of the 18 variants could not be functionally analyzed because they did not conduct sufficient sodium currents. 5 variants did not generate any sodium current in oocytes. Among them, BgNa$_v$20 contained a premature stop codon caused by the exclusion of optional exon A. BgNa$_v$12, BgNa$_v$13, and BgNa$_v$14 lacked exon K (encoding IS2-3). BgNa$_v$19 contained two mutually exclusive exons, G1 and G2. It is likely that introduction of a premature stop codon in BgNa$_v$20, missing part of transmembrane segment IS2-3 (exon K) in BgNa$_v$12, BgNa$_v$13, and BgNa$_v$14, or having an extra transmembrane segment (exons G1 and G2) in IIIS3-4 in BgNa$_v$19 are responsible for nonfunctional channels in oocytes. The remaining four variants, BgNa$_v$15, BgNa$_v$16, BgNa$_v$17, and BgNa$_v$18, however, did not have any stop codon or missing transmembrane segments, but the peak current amplitude for these variants was less than 0.5 μA 1 week after injection of 2 ng of cRNA/oocyte, which was not sufficient for functional analysis. Comparison of alternative exon usage revealed that all four variants contained exon B, which encodes an 8-amino acid sequence in the first linker connecting domains I and II (Fig. 1*A*).

To determine whether inclusion of exon B is responsible for poor expression of sodium current in these variants, we deleted exon B from variants BgNa$_v$15 and BgNa$_v$16. The resultant recombinant construct produced robust expression of sodium currents (Fig. 2). Furthermore, when we inserted exon B into

[1] Domains are designated with Roman numerals and segments within the domains with Arabic numbers; for example IS2-3 is domain I, segment 2-3.

TABLE II
Functional properties of nine splice variants

The voltage dependence of activation and inactivation was fitted with two-state Boltzmann equations, as described under "Experimental Procedures," to determine $V_{1/2}$, the voltage for half-maximal conductance or inactivation, and k, the slope factor for conductance or inactivation. Each value represents the mean ± S.D. for at least five oocytes.

	Activation		Fast inactivation		Recovery from inactivation			
	$V_{1/2}$	k	$V_{1/2}$	k	τ_1	A_1	τ_2	A_2
	mV		*mV*		*ms*	*%*	*ms*	*%*
$BgNa_v1$-2	−24.9 ± 1.4	4.9 ± 0.4	−49.0 ± 0.7	4.8 ± 0.2	0.8 ± 0.1	86 ± 2	49 ± 9	14 ± 2
$BgNa_v5$	−25.5 ± 0.9	4.8 ± 0.4	−45.5 ± 0.9	4.3 ± 0.1	0.7 ± 0.1	90 ± 2	28 ± 7	10 ± 2
$BgNa_v6$	−27.4 ± 6.2	4.0 ± 1.0	−38.7 ± 1.8	4.2 ± 0.2	0.6 ± 0.1	93 ± 3	38 ± 4	7 ± 3
$BgNa_v7$	−29.2 ± 3.8	4.1 ± 0.5	−44.9 ± 1.8	4.4 ± 0.2	0.6 ± 0.1	90 ± 4	18 ± 5	10 ± 4
$BgNa_v8$	−30.1 ± 4.4	5.4 ± 0.5	−54.4 ± 1.4	5.6 ± 0.1	0.8 ± 0.0	89 ± 1	35 ± 6	11 ± 1
$BgNa_v9$	−30.6 ± 3.9	4.2 ± 0.7	−49.3 ± 0.6	4.1 ± 0.1	1.3 ± 0.2	90 ± 2	24 ± 8	10 ± 2
$BgNa_v1$-3	−34.1 ± 4.4	4.3 ± 0.4	−48.4 ± 0.8	4.6 ± 0.1	0.6 ± 0.1	89 ± 3	26 ± 3	11 ± 3
$BgNa_v10$	−36.7 ± 3.4	1.9 ± 0.6	−37.2 ± 0.9	3.7 ± 0.1	0.5 ± 0.0	95 ± 1	24 ± 5	5 ± 1
$BgNa_v11$	−43.9 ± 3.0	4.7 ± 0.8	−54.0 ± 1.5	4.5 ± 0.2	0.6 ± 0.1	94 ± 1	70 ± 12	6 ± 1

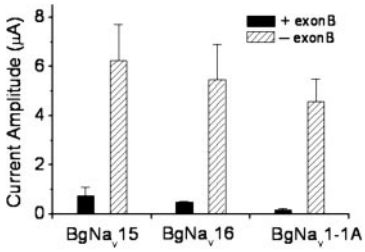

FIG. 2. **Optional exon B modulates sodium current expression.** Both $BgNa_v15$ and $BgNa_v16$ contain exon B. Deletion of exon B in $BgNa_v15$ and $BgNa_v16$ increases the amplitude of peak current. $BgNa_v1$-1A lacks exon B. Addition of exon B into $BgNa_v1$-1A reduces the amplitude of peak current. The peak current was measured by a 20-ms depolarization to −10 mV from the −120-mV holding potential at day 4 after injection of 0.2 ng of cRNA for $BgNa_v1$-1A and its recombinant, and 2 ng of cRNA for $BgNa_v15$, $BgNa_v16$, and their recombinants.

functional $BgNa_v1$-1A, which is identical in sequence to published $BgNa_v$ (accession number U73583), the amplitude of peak current of the recombinant channels was greatly reduced (Fig. 2). These complementary results demonstrated that exon B modulates sodium channel expression and/or function. However, one exon B-containing variant, $BgNa_v10$, produced sufficient sodium currents (greater than 0.5 μA in amplitude) for functional analysis. We hypothesize that an unidentified sequence(s) in $BgNa_v10$ counteracted the negative regulation of sodium current expression by exon B.

L1285P in $BgNa_v1$-1 Alters the Voltage Dependence of Activation and Steady-state Inactivation—In addition to different alternative exon usage, sequence analysis of the 9 functional variants revealed on average five scattered amino acid changes compared with the published $BgNa_v$ sequence (31; GenBank accession number U73583) (Table III). We next examined a possible contribution of these amino acid differences to the observed differences in gating properties among variants.

Both $BgNa_v1$-1 and $BgNa_v1$-2 activate at about 10 mV more depolarizing potentials than other variants. $BgNa_v1$-1 possesses four amino acid changes compared with the published sequence (Table III). Using site-directed mutagenesis, we individually changed these four residues in $BgNa_v1$-1 to the corresponding residues in the published $BgNa_v$ sequence, producing four recombinant channels, G502R, P1285L, A1685V, and L1806I (*e.g.* for G502R: changing Gly in $BgNa_v1$-1 to Arg in the published sequence). Compared with the parental channel $BgNa_v1$-1, P1285L reverted the voltage dependence of activation by about 10 mV in the hyperpolarizing direction (Fig. 3 and Table IV). It also caused a 5-mV hyperpolarizing shift in the voltage dependence of steady-state inactivation (Fig. 3 and Table IV). The other three substitutions caused a subtle (3–4-mV) hyperpolarizing shift in activation but no effect on inactivation (Fig. 3 and Table IV). Therefore, Pro^{1285} in $BgNa_v1$-1 appears to be responsible for the large depolarization-required activation of the $BgNa_v1$-1 channel.

L1285P and V1685A Are the Result of Tissue-specific U-to-C Editing—The L1285P change in $BgNa_v1$-1 resulted from a nucleotide change from T^{3854} to C^{3854}. To examine whether this change is the result of RNA editing, we amplified an ~300-bp cDNA, which contains the L1285P change, using primers 16 and 17 and cDNA from heads/thorax, ovary, or gut (Fig. 4). Because the Leu (CTC) to Pro (CCC) change created a recognition site, CCCGC$(N)_4$, for restriction enzyme FauI, we were able to determine the presence of T or C in the isolated clones by restriction enzyme digestion. All 46 clones isolated from head/thorax had a T at nucleotide 3854. However, we identified two types of clones from ovary and gut. Although most of the clones contain a T, 6 of 28 clones from ovary and 3 of 20 clones from gut contained a C at nucleotide 3854. An ~2.8-kb PCR fragment was amplified using the same PCR primer pair (primers 16 and 17) and genomic DNA as the template. Sequencing of the 2.8-kb fragment revealed a T at the corresponding position. Therefore, the Leu to Pro change in IIIS1 resulted from a U-to-C editing event, and this editing occurs only in ovary and gut. By convention, this editing site is designated as Leu/Pro site. Previous studies showed that when both edited and unedited transcripts were produced, direct sequencing of the reverse transcription-PCR products could sometimes result in mixed sequence signals in the chromatogram (29). We used direct sequencing of the reverse transcription-PCR product and found a double peak signal at the Leu/Pro site in ovary and gut but a single peak in nerve cord and leg of the same cockroach individuals (Fig. 5, *A–D*), further confirming that the Leu/Pro editing event is tissue-specific.

In $BgNa_v1$-1, V1685A is also caused by a T^{5054} to C^{5054} change. To determine whether V1685A also resulted from U-to-C editing, we amplified a 213-bp fragment encoding IVS2–IVS4 using primers 18 and 19. We found a double peak signal, C^{5054} and T^{5054}, in a fragment amplified from ovary and gut (Fig. 5, *F* and *G*). However, a single sequence signal (T) was found in nerve cords and legs of the same cockroach individuals (Fig. 5, *H* and *I*). Furthermore, a T corresponding to T^{5054} was found in a 7-kb genomic DNA amplified using the same PCR primer pair (Fig. 5*J*). Therefore, we identified a second U-to-C editing site, resulting in a Val to Ala change in IVS4, designated as the Val/Ala site. Both the L1285P and V1685A changes were detected in ovary and gut, but not in the nerve cord or leg. Therefore, $BgNa_v1$-1 is an ovary- and gut-specific variant.

Identification of Two A-to-I Editing Sites in $BgNa_v$—$BgNa_v1$-2 possesses four amino acid changes, R45G, K184R, I1663M, and N1787D, compared with the available sequence (Table III). I1663M, resulting from an A^{4989} to G^{4989} change,

TABLE III
Scattered amino acid changes in BgNa$_v$ variants
The amino acid positions refer to those in the published sequence of BgNa$_v$ (GenBank accession number U73583).

BgNa$_v$1-1	R502G	L1285P	V1685A	I1806L				
BgNa$_v$1-2	R45G	K184R	I1663M	N1798D				
BgNa$_v$1-3	L453V	F396L	V1223A	M1637V	I1663M	I1899T		
BgNa$_v$5	R45G	V106M	K425R	Q694R	S1143G	I1663M		
BgNa$_v$6	M955V	S1143G	I1488M	I1663M	V1693A			
BgNa$_v$7	F143L	F821S	N1019D	F1028S	I1663M	T1915A		
BgNa$_v$8	R45G	F157S	H554Y	I630R	A823T	G1162R	E1649G	R1686G
BgNa$_v$9	V75A	A414T	N795D	F820S	A1288P	L1348H	K1674R	D2030N
BgNa$_v$10	R564G	D688G	S1032P	N1485S	I1663M	S1633A		
BgNa$_v$11	H635L	F1627L	P1679S	G1842S				

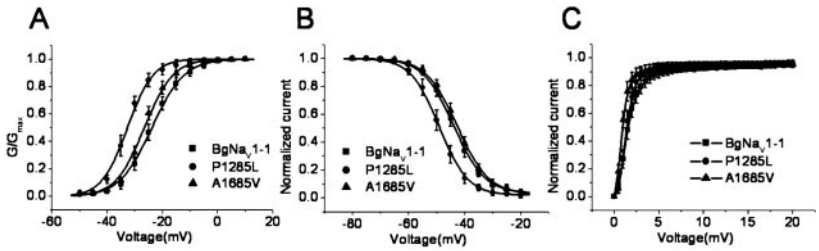

FIG. 3. **P1285L shifted the voltage dependence of activation and inactivation in the hyperpolarizing direction.** The voltage dependence of activation (*A*), steady-state inactivation (*B*), and recovery from fast inactivation (*C*) were compared between BgNa$_v$1-1 and its two recombinant channels, P1285L (*i.e.* from Pro in BgNa$_v$1-1 to Leu in the available sequence) and A1685V. The recording protocols are described under "Experimental Procedures." *Symbols* represent means; *error bars* represent S.D. values from at least nine oocytes.

TABLE IV
Gating properties of BgNa$_v$1-1 and its mutants
The voltage dependence of conductance and inactivation was fitted with two-state Boltzmann equations, as described under "Experimental Procedures," to determine $V_{1/2}$, the voltage for half-maximal conductance or inactivation, and k, the slope factor for conductance or inactivation. Each value represents the mean ± S.D. for at least six oocytes. *Statistically significant difference compared with BgNa$_v$1-1 ($p < 0.05$). **Statistically significant difference compared with BgNa$_v$1-1 ($p < 0.01$)

	Activation		Inactivation	
	$V_{1/2}$	k	$V_{1/2}$	k
	mV		*mV*	
BgNa$_v$1–1	−23.7 ± 1.8	5.4 ± 0.7	−43.7 ± 1.2	5.2 ± 0.2
G502R	−27.4* ± 1.1	5.3 ± 0.3	−43.7 ± 0.7	4.8 ± 0.4
P1285L	−32.6** ± 1.3	4.1 ± 1.0	−48.9** ± 1.4	4.7 ± 0.2
A1685V	−26.4* ± 1.8	4.7 ± 0.9	−42.4 ± 1.1	5.3 ± 0.3
L1806I	−26.6* ± 1.9	5.5 ± 0.6	−44.5 ± 0.9	5.2 ± 0.2

was found in 6 of the 9 sequenced full-length cDNA clones (Table III). PCR analysis of the remaining clones using a sequence-specific primer revealed that 49 of 69 clones contain G^{4989} and the remaining 20 possess A^{4989}. To determine whether I1663M is caused by RNA editing, we amplified a 213-bp fragment encoding IVS2–IVS4, where A^{4989} is located, using primers 18 and 19 and RNA isolated from head/thorax. Sequencing of the PCR fragment revealed the mixed A and G signal at nucleotide 4989 (Fig. 5*A*). To determine whether the mixed A and G signal was present in BgNa$_v$ transcripts expressed in various tissues, we amplified the same region using RNA from nerve cord, leg, ovary, and gut and sequenced the PCR products. A double A and G signal was detected in nerve cord and leg (Fig. 5, *A* and *B*), but a single G was found in ovary and gut (Fig. 5, *C* and *D*). Furthermore, genomic DNA sequencing revealed an A at the corresponding position (Fig. 5*E*). Collectively, these results demonstrated that the A^{4989} to G^{4989} change was caused by an A-to-I RNA editing, resulting in an amino acid change from an Ile^{1663} to an Met^{1663} in IVS3. We designated this site as the Ile/Met site, the first A-to-I RNA editing site in the German cockroach sodium channel.

In addition to its tissue-specific regulation, this A-to-I RNA editing event was also regulated developmentally. We examined the developmental profile of edited and unedited transcripts in five developmental stages, three embryonic stages (I, II, and III) and two immature stages (nymph I and II). Sequencing analysis showed that the unedited transcript (carrying A^{4989}), but not the edited one (carrying G^{4989}), was found in the embryonic stage I, during which no cellular differentiation had occurred yet (Fig. 5*F*). Both unedited and edited transcripts were present in the rest of the development stages (Fig. 5, *G–J*). These results indicate the A^{4989} to G^{4989} editing event is initiated in the embryo, probably concurrent with the development of the nervous system.

To determine whether K184R is the result of RNA editing, we amplified a 216-bp fragment encoding IS1 to IS2 using primers 20 and 21. A total of 70 cDNA clones were isolated and the inserts sequenced. One of 70 clones contained a G^{551}, which resulted in a Lys (AAG) to Arg (AGG) change in the amino acid sequence. The remaining 69 clones contain an A^{551}. We sequenced the corresponding genomic PCR fragment amplified using the same primer pair. The nucleotide A was present in the genomic DNA. No alternative exon containing T was found. Therefore, we identified a possibly second A-to-I editing resulting in the K184R change in the cockroach sodium channel transcript. This editing site is designated as the Lys/Arg site. This RNA editing appears to occur at a low frequency compared with the Ile/Met editing site.

The remaining two amino acid changes, R45G and N1787D, in BgNa$_v$1-2 are both caused by an A to G change. For N1787D, we isolated 75 partial cDNA clones from head and thorax tissues. Sequence analysis revealed an A in all 75 partial cDNA

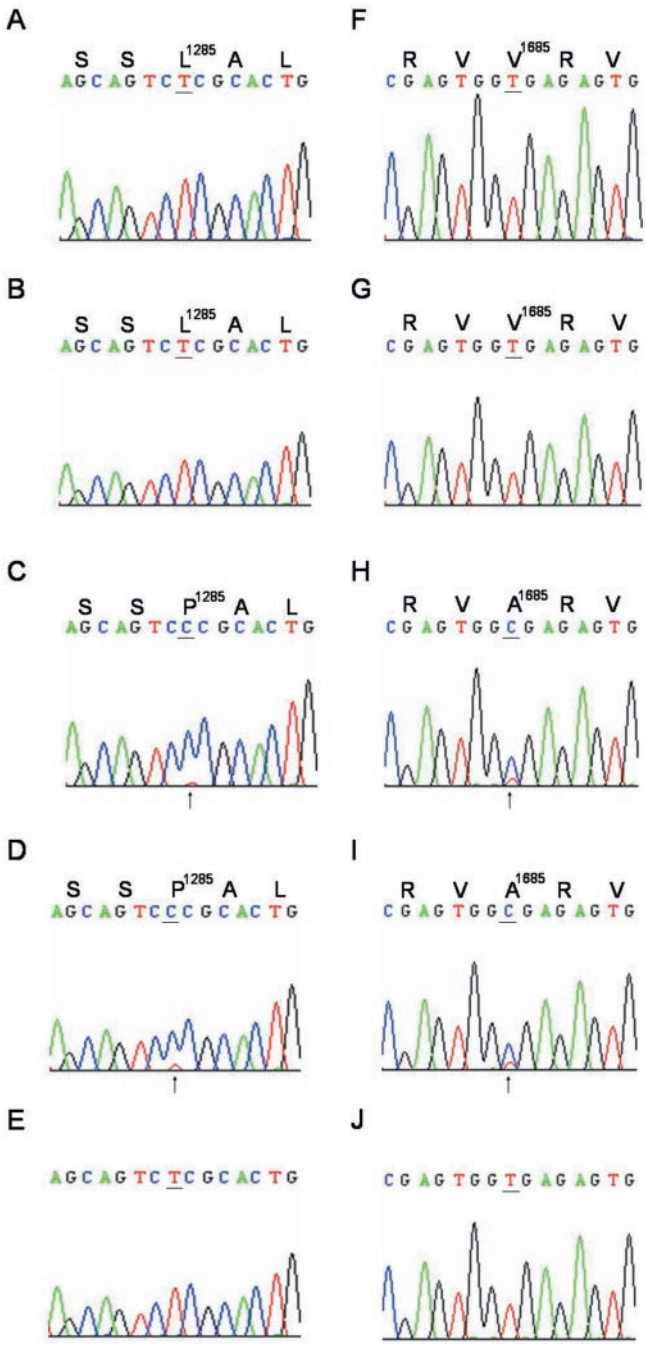

FIG. 4. **Tissue-specific editing of Leu/Pro and Val/Ala sites.** Sequence analysis reveals single or double peak signals at the editing sites (*underlined*) in four tissues: nerve cord (*A* and *F*), leg (*B* and *G*), ovary (*C* and *H*), and gut (*D* and *I*) at the Leu/Pro and Val/Ala sites. Deduced amino acid sequences and the locations of the editing sites are indicated above the nucleotide sequences. The nucleotide sequences from genomic DNA are shown in *E* and *J*. The double peaks T and C (indicated by *arrowheads*) are detected in ovary and gut for both Leu/Pro and Val/Ala sites.

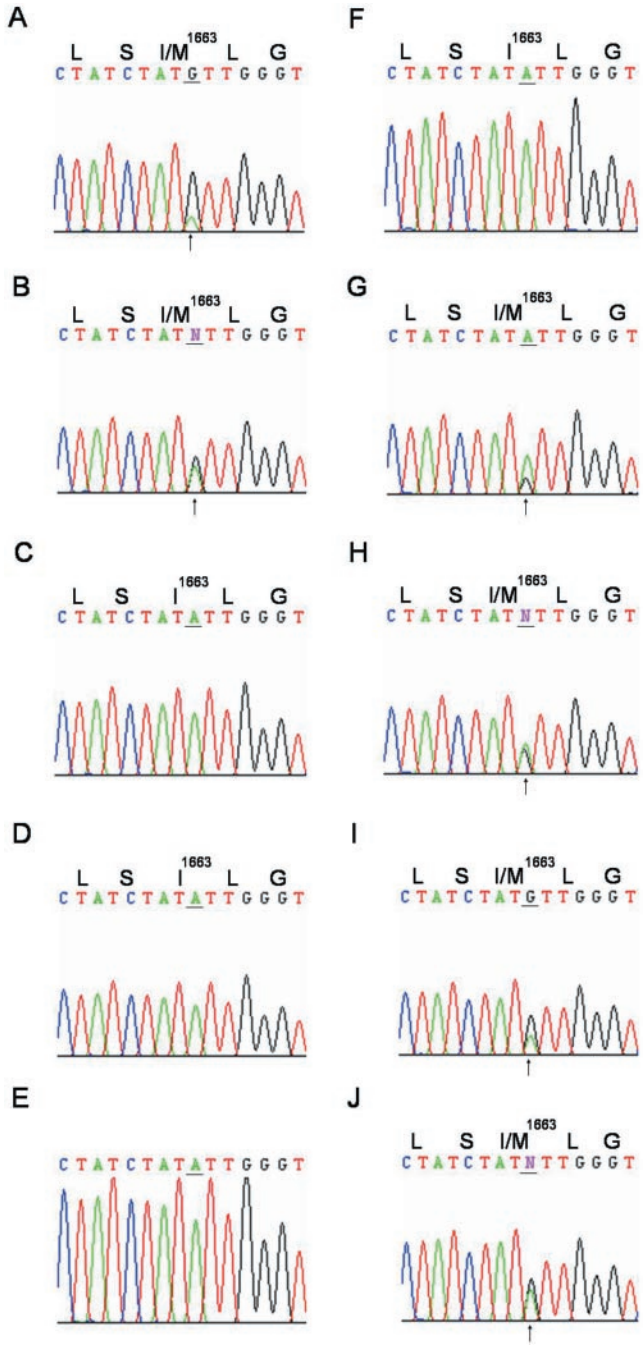

FIG. 5. **Tissue-specific and development-specific editing of the Ile/Met site.** Sequence analysis reveals single or double peak signals at the Ile/Met site in four tissues: nerve cord (*A*), leg (*B*), ovary (*C*), and gut (*D*), and five developmental stages: embryonic I (*F*), II (*G*) and III (*H*); nymphal I (*I*) and II (*J*). Deduced amino acid sequences and the locations of the editing sites are indicated above the nucleotide sequences. The nucleotide sequence from genomic DNA is shown in *E*. The double peaks A and G are indicated by *arrows*.

clones. Therefore, whether N1787D is caused by an A-to-I editing event could not be ascertained. It could be because of a PCR error in the amplification of full-length cDNA clones. On the other hand, R45G was present not only in $BgNa_v1$-2 but also in variant $BgNa_v5$ with a completely different exon usage. Therefore, it is likely caused by an A-to-I editing. Thus, we identified two A-to-I editing events in $BgNa_v1$-2, which resulted in Ile to Met and Lys to Arg changes. We suggest that R45G is also generated from an A-to-I editing. Because of low frequencies of K184R and R45G, future larger scale analysis may be needed to substantiate the conclusion of the generation of these two changes by A-to-I RNA editing.

K184R Is Responsible for the Distinct Gating Properties of $BgNa_v1$-2—To determine which amino acid change is responsible for the requirement of more membrane depolarization for activation of $BgNa_v1$-2, we individually changed the amino acid residues and examined the mutant channel gating properties. The Arg to Lys substitution reverted the voltage dependence of activation by 7 mV in the hyperpolarizing direction, indicating that Arg^{184} is responsible for the more depolarization-required activation of the $BgNa_v1$-2 channel. None of the other muta-

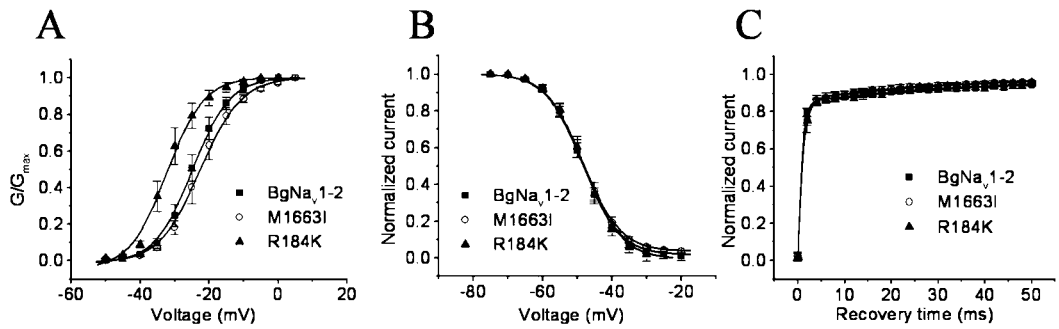

FIG. 6. **R184K shifted the voltage dependence of activation in the hyperpolarizing direction.** The voltage dependence of activation (*A*), steady-state inactivation (*B*), and recovery from fast inactivation (*C*) were compared between BgNa$_v$1-2 and its two single-amino acid substitutions derivatives, R184K (*i.e.* from Arg in BgNa$_v$1-2 to Lys in the available sequence) and M1663I. The recording protocols are described under "Experimental Procedures." *Symbols* represent means; *error bars* represent S.D. values from at least eight oocytes.

tions altered the gating properties, including voltage-dependent activation, steady-state inactivation, and recovery from fast inactivation (Fig. 6 and Table V).

DISCUSSION

In this study, we identified 20 splice types of the cockroach sodium channel BgNa$_v$. The electrophysiological characterization of these variants in *Xenopus* oocytes revealed an impressive spectrum of differences in the level of sodium current expression and the voltage-dependent activation and/or inactivation among cockroach sodium channel variants. We found that exclusion or inclusion of an optional exon, exon B, modulates the sodium current expression. We identified two A-to-I RNA editing sites and two U-to-C editing sites, each resulting in amino acid changes in transmembrane segments. Two of these editing events significantly alter the voltage dependence of activation and/or inactivation. Furthermore, these RNA editing events occur only in specific tissues, generating tissue-specific insect sodium channels. Thus, this study not only represents a comprehensive functional characterization of sodium channel variants in insects, but also provides the first direct evidence for the involvement of RNA editing in modification of sodium channel gating properties.

Functional Complexity of Insect Sodium Channel Variants—Results presented here clearly suggest that a high level of functional plasticity of a sodium channel can be generated from a single gene via post-transcriptional modifications. For example, BgNa$_v$11 activates at more negative membrane potentials, *e.g.* −60 mV, whereas others require more membrane depolarization, such as −45 mV, for channel activation. Similarly, the half-maximal voltages for the voltage dependence of steady-state inactivation range from −37 to −60 mV. BgNa$_v$7 has a significant overlap between the voltage dependence of activation and the voltage dependence of steady-state inactivation, with $V_{½}$ values of −36.7 and −37.2 mV for activation and inactivation, respectively. Consequently, this variant produces a large window current over a range of −45 mV to −25 mV, which could lead to membrane depolarization at subthreshold potentials, resulting in oscillatory activities, summation of synaptic input, or controlling firing frequency, and so on (32). Thus, even though insects carry only a single sodium channel gene, a combination of alternative splicing and RNA editing of the primary transcript can apparently produce a full complement of functionally diverse sodium channels. It is therefore likely that mammals have evolved to rely on multiple sodium channel genes to produce functionally distinct isoforms, whereas insects must depend on extensive alternative splicing and RNA editing of a single sodium channel gene to fulfill specialized roles of sodium channel activity in different cell types/tissues.

Alternative Exon B Modulates Sodium Current Expression—Significant variation in the amplitude of peak current was recorded from sodium channels in *Drosophila* embryonic neurons (33). Single cell reverse transcription-PCR and recording analysis by O'Dowd and associates (19) showed that exon a in *Drosophila para* is necessary but not sufficient for the expression of sodium current in cultured embryonic neurons. However, Warmke *et al.* (9) reported no significant difference in sodium current expression and gating properties between *para* splice variants with or without exon a. In this study, we observed poor sodium current expression of variants containing exon B (equivalent to exon b in *Drosophila para*) (Fig. 3). Exon swapping experiments showed that exclusion of exon B is critical for robust expression of sodium currents in oocytes. Considering that the location and sequence of this exon are highly conserved in *Drosophila para* (Fig. 1*A*) and also in house fly *Vssc1* (21), the role of exon b/B in regulating insect sodium current expression may be universal. Down-regulation of sodium current expression by protein kinases has been documented for mammalian sodium channels (34–38). Because exon B is located in the first intracellular linker and contains a consensus sequence for phosphorylation, this exon could serve as a regulatory on-or-off switch regulating the neuronal excitability by responding to second messengers or G protein-coupled modulation signals to meet unique physiology in given tissues or cell types. Interestingly, we found that one splice variant, BgNa$_v$7-1, also contains exon B yet produced detectable sodium currents in oocytes, suggesting the involvement of additional sequences in modulating sodium current expression.

Both A-to-I and U-to-C RNA Editing Contributes to Sodium Channel Functional Diversity—Among all RNA editing types, A-to-I editing is the most prevalent one found in the nervous system (see below), whereas U-to-C editing is reported only in a very few transcripts in animals (39–41). About a dozen transcripts encoding ion channels, neurotransmitter receptors, or G protein-coupled receptors are substrates of A-to-I editing.

TABLE V
Gating properties of BgNa$_v$1-2 and its mutants

The voltage dependence of conductance and inactivation was fitted with two-state Boltzmann equations, as described under "Experimental Procedures," to determine $V_{1/2}$, the voltage for half-maximal conductance or inactivation, and *k*, the slope factor for conductance or inactivation. Each value represents the mean ± S.D. for at least five oocytes. *Statistically significant difference compared with BgNa$_v$1-2 ($p < 0.05$).

	Activation		Inactivation	
	$V_{1/2}$	*k*	$V_{1/2}$	*k*
	mV		*mV*	
BgNa$_v$1-2	−24.9 ± 1.4	4.9 ± 0.4	−49.0 ± 0.7	4.8 ± 0.2
G45R	−24.8 ± 2.4	4.9 ± 0.4	−47.1 ± 1.5*	5.0 ± 0.2
R184K	−31.8 ± 2.4*	4.2 ± 0.5	−48.3 ± 1.0	4.7 ± 0.1
M1663I	−23.4 ± 1.8	5.2 ± 0.4	−49.0 ± 1.5	4.9 ± 0.1
D1798N	−22.3 ± 1.9	5.4 ± 0.7	−48.2 ± 1.1	4.8 ± 0.3

The well characterized examples include A-to-I editing in mammalian glutamate-gated receptor channels, which mediate excitatory synaptic transmission in the central nervous system (42 and refs. therein), mammalian serotonin 2C receptor (25, 26), and squid voltage-gated potassium channels (27, 28). In each case, edited channels or receptors exhibit distinct functional and/or pharmacological properties. For example, A-to-I editing at a Gln/Arg site of the Glu receptor subunit B RNA results in a drastic decrease in the Ca^{2+} permeability of subunit B-containing Glu receptor (43). Editing at an Arg/Glu site, by contrast, results in faster recovery rates from Glu receptor channel desensitization (44). A-to-I editing in serotonin 2C receptor transcripts reduces the affinity of the receptor for its G protein (25). Extensive A-to-I editing of potassium channel mRNAs generates functionally distinct channels and regulates subunit tetramerization (27, 28). A-to-I editing has also been reported in several transcripts in the nervous system of *D. melanogaster*: a Ca^{2+} channel α1 subunit (45), a glutamate-gated Cl^- channel (46), the *para* sodium channel (47, 48), and subunits of a putative nicotinic acetylcholine receptor (49). 10 A-to-I editing sites have been reported in the *para* transcript (47, 48). However, the functional consequences of A-to-I editing in *para* remain elusive prior to this study.

Here, we identified two novel U-to-C editing sites, Leu/Pro and Val/Ala, in $BgNa_v1$-1 causing the L1285P change in IIIS1 and the V1685A change in IVS4. We also identified two novel A-to-I editing sites in $BgNa_v1$-2, Lys/Arg and Ile/Met, resulting in the K184R change in IS2 and the I1663M change in IVS3. Both $BgNa_v1$-1 and $BgNa_v1$-2 activate at about 10 mV more depolarizing potentials than other variants. Furthermore, $BgNa_v1$-1 also inactivates at about 10 mV more depolarizing potentials than other variants. Our site-directed mutagenesis results showed that eliminating the U-to-C editing at the Leu/Pro site rendered $BgNa_v1$-1 to activate and inactivate at more hyperpolarizing membrane potentials. Similarly, abolishment of the A-to-I editing at the Lys/Arg site shifted the voltage dependence of activation of $BgNa_v1$-2 a more hyperpolarizing potential. Clearly, these editing events are responsible for more-depolarization-required activation of $BgNa_v1$-1 and $BgNa_v1$-2. The modification of sodium channel gating properties by RNA editing supports the notion that one major role of RNA editing is the fine tuning of the neuronal activity (23).

RNA editing at the Ile/Met and Val/Ala sites did not alter any sodium channel gating properties. However, both editing events were regulated in a tissue-specific manner. In fact, RNA editing at the Ile/Met site occurs in a high frequency. The importance of these two editing events remains unclear. It is possible that the effects of these RNA editing events require additional cellular signals present only in specific tissues/cell type, but absent in *Xenopus* oocytes.

Tissue-specific RNA Editing—We show that the Leu/Pro and Val/Ala editing events occur only in ovary and gut. Tissue-specific regulation of RNA editing events suggests a more specialized role of edited channels in specific tissues or cell types. $BgNa_v1$-1, edited at both Leu/Pro and Val/Ala sites, therefore represents an ovary- and gut-specific variant. $BgNa_v1$-1 may be expressed in neurons that innervate the ovary and gut. Because $BgNa_v1$-1 and $BgNa_v1$-2 activate at more depolarizing potentials than other variants, neurons expressing these variants would have a higher threshold for firing action potentials and a decrease in neuronal excitability compared with neurons expressing the unedited variants.

In summary, we demonstrated here the extraordinary ability of a single insect sodium channel gene to produce a wide array of sodium channels with distinct functional properties. We found that, in addition to alternative splicing, RNA editing is a major mechanism for increasing sodium channel functional plasticity. Understanding the physiological roles of different alternatively spliced and/or RNA-edited sodium channel variants in insects and the mechanisms by which tissue-/cell type-specific splicing and RNA editing are controlled is clearly important for future research.

Acknowledgments—We thank Drs. Dalia Gordon, Noah Koller, and Vincent Salgado for critical review of an early version of this manuscript and Michelle Carlson for editorial assistance.

REFERENCES

1. Catterall, W. A. (2000) *Neuron* **26,** 13–25
2. Goldin, A. L., Barchi, R. L., Caldwell, J. H., Hofmann, F., Howe, J. R., Hunter, J. C., Kellen, R. G., Mandel, G., Meisler, M. H., Netter, Y. B., Noda, M., Tamkun, M. M., Waxman, S. G., Wood, J. N., and Catterall, W. A. (2000) *Neuron* **28,** 365–368
3. Catterall, W. A., Goldin, A. L., and Waxman, S. G. (2003) *Pharmacol. Rev.* **55,** 575–578
4. Goldin, A. L. (2001) *Annu. Rev. Physiol.* **63,** 871–894
5. Dib-Hajj, S. D., Black, J. A., Cummins, T. R., and Waxman, S. G. (2002) *Trends Neurosci.* **25,** 253–259
6. Yu, F. H., and Catterall, W. A. (2003) *Genome Biol.* **4,** 207.1–207.7
7. Loughney, K., Kreber, R., and Ganetzky, B. (1989) *Cell* **58,** 1143–1154
8. Feng, G., Deak, P., Chopra, M., and Hall, L. M. (1995) *Cell* **82,** 1001–1011
9. Warmke, J. W., Reenan, R. A. G., Wang, P., Qian, S., Arena, J. P., Wang, J., Wunderler, D., Liu, K., Kaczorowski, G. J., Van Der Ploeg, L. H. T., Ganetzky, B., and Cohen, C. J. (1997) *J. Gen. Physiol.* **110,** 119–133
10. Smith, T. J., Lee, S. H., Ingles, P. J., Knipple, D. C., and Soderlund, D. M. (1997) *Insect Biochem. Mol. Biol.* **27,** 807–812
11. Tan, J., Liu, Z., Tsai, T.-D., Valles, S. M., Goldin, A. L., and Dong, K. (2002) *Insect Biochem. Mol. Biol.* **32,** 445–454
12. Tan, J., Liu, Z., Nomura, Y., Goldin, A. L., and Dong, K. (2002) *J. Neurosci.* **22,** 5300–5309
13. Sarao, R., Gupta, S. K., Auld, V. J., and Dunn, R. J. (1991) *Nucleic Acids Res.* **19,** 1873–1879
14. Schaller, K. L., Krzemien, D. M., McKenna, N. M., and Caldwell, J. H. (1992) *J. Neurosci.* **12,** 1370–1381
15. Gustafson, T. A., Clevinger, E. C., O'Neill, T. J., Yarowsky, P. J., and Krueger, B. K. (1993) *J. Biol. Chem.* **268,** 18648–18653
16. Thackeray, J. R., and Ganetzky, B. (1994) *J. Neurosci.* **14,** 2569–2578
17. Thackeray, J. R., and Ganetzky, B. (1995) *Genetics* **141,** 203–214
18. O'Dowd, D. K., Gee, J. R., and Smith, M. A. (1995) *J. Neurosci.* **15,** 4005–4012
19. Dietrich, P. S., McGivern, J. G., Delgado, S. G., Koch, B. D., Eglen, R. M., Hunter, J. C., and Sangameswaran, L. (1998) *J. Neurochem.* **70,** 2262–2272
20. Plummer, N. W., McBurney, M. W., and Meisler, M. H. (1997) *J. Biol. Chem.* **272,** 24008–24015
21. Lee, S. H., Ingles, P. J., Knipple, D. C., and Soderlund, D. M. (2002) *Invert. Neurosci.* **4,** 125–133
22. Bass, B. L. (2001) *RNA Editing*, Oxford University Press, Oxford
23. Seeburg, P. H. (2000) *Neuron* **25,** 261–263
24. Seeburg, P. H. (2002) *Neuron* **35,** 17–20
25. Burns, C. M., Chu, H., Rueter, S. M., Hutchison, L. K., Canton, H., Sanders-Bush, E., and Emeson, R. B. (1997) *Nature* **387,** 303–308
26. Niswender, C. M., Copeland, S. C., Herrick-Davis, K., Emeson, R. B., and Sanders-Bush, E. (1999) *J. Biol. Chem.* **274,** 9472–9478
27. Patton, D. E., Silva, T., and Bezanilla, F. (1997) *Neuron* **19,** 711–722
28. Rosenthal, J. J. C., and Bezanilla, F. (2002) *Neuron* **34,** 743–757
29. Palladino, M. J., Keegan, L. P., O'Connell, M. A., and Reenan, R. A. (2000) *Cell* **102,** 437–449
30. Bell, W. L. (1981) *The Laboratory Cockroach*, Chapman and Hall, New York
31. Dong, K. (1997) *Insect Biochem. Mol. Biol.* **27,** 93–100
32. Crill, W. E. (1996) *Annu. Rev. Physiol.* **58,** 349–362
33. Byerly, L., and Leung, H. (1988) *J. Neurosci.* **8,** 4379–4393
34. Numann, R., Catterall, W. A., and Scheuer, T. (1991) *Science* **254,** 115–118
35. West, J. W., Numann, R., Murphy, B. J., Scheuer, T., and Catterall, W. A. (1991) *Science* **254,** 866–868
36. Smith, R. D., and Goldin, A. L. (1996) *J. Neurosic.* **16,** 1965–1974
37. Smith, R. D., and Goldin, A. L. (1997) *J. Neurosci.* **17,** 6066–6093
38. Smith, R. D., and Goldin, A. L. (2000) *Am. J. Physiol. Cell Physiol.* **278,** C638–C645
39. Nagalla, S. R., Barry, B. J., and Spindel, E.R. (1994) *Mol. Endocrinol.* **8,** 943–951
40. Sharma, P. M., Bowman, M., Madden, S. L., Rauscher, F. J., III, and Sukumar, S. (1994) *Genes Dev.* **8,** 720–731
41. Villegas, J., Muller, I., Arredondo, J., Pinto, R., and Burzio, L. (2002) *Nucleic Acids Res.* **30,** 1895–1901
42. Seeburg, P. H., Higuchi, M., and Sprengel, R. (1998) *Brian Res. Rev.* **26,** 217–229
43. Sommer, B., Kohler, M., Sprengel, R., and Seeburg, P. H. (1991) *Cell* **67,** 11–19
44. Lomeli, H., Mosbacher, J., Melcher, T., Hoger, T., Geiger, J. R., Kunker, T., Monyer, H., Higuchi, M., Bach, A., and Seeburg, P. H. (1994) *Science* **266,** 1709–1713
45. Smith, L. A., Peixoto, A. A., and Hall, J. C. (1998) *J. Neurogenet.* **12,** 227–240
46. Semenov, E. P., and Park, W. L. (1999) *J. Neurochem.* **72,** 66–72
47. Reenan, R. A., Nanrahan, C. J., and Ganetzky, B. (2000) *Neuron* **25,** 139–149
48. Hanrahan, C. J., Palladino, M. J., Ganetzky, B., and Reenan, R. A. (2000) *Genetics* **155,** 1149–1160
49. Grauso, M., Reenan, R. A., Culetto, E., and Sattelle, D. B. (2002) *Genetics* **160,** 1519–1533